AD_____

Award Number: DAMD17-00-1-0303

TITLE: Construction of Affinity Probes to Study the Epothilone Binding Site on Tubulin

PRINCIPAL INVESTIGATOR: Emily A. Reiff
Mentor: Gunda I. Georg, Ph.D.

CONTRACTING ORGANIZATION: University of Kansas Center for Research, Inc.
Lawrence, KS 66044-7552

REPORT DATE: May 2003

TYPE OF REPORT: Annual Summary

PREPARED FOR: U.S. Army Medical Research and Materiel Command
Fort Detrick, Maryland 21702-5012

REPORT DOCUMENTATION PAGE

Form Approved
OMB No. 074-0188

1. AGENCY USE ONLY (Leave blank)	2. REPORT DATE	3. REPORT TYPE AND DATES COVERED
	May 2003	Annual Summary (15 Apr 2000 - 14 Apr 2003)

4. TITLE AND SUBTITLE
Construction of Affinity Probes to Study the Epothilone Binding Site on Tubulin

5. FUNDING NUMBERS
DAMD17-00-1-0303

6. AUTHOR(S)
Emily A. Reiff
Mentor: Gunda I. Georg, Ph.D.

7. PERFORMING ORGANIZATION NAME(S) AND ADDRESS(ES)
University of Kanasas Center for Research, Inc.
Lawrence, KS 66044-7552

E-Mail: reiff@falcon.cc.ukans.edu

8. PERFORMING ORGANIZATION REPORT NUMBER

9. SPONSORING / MONITORING AGENCY NAME(S) AND ADDRESS(ES)
U.S. Army Medical Research and Materiel Command
Fort Detrick, Maryland 21702-5012

10. SPONSORING / MONITORING AGENCY REPORT NUMBER

11. SUPPLEMENTARY NOTES

12a. DISTRIBUTION / AVAILABILITY STATEMENT
Approved for Public Release; Distribution Unlimited

12b. DISTRIBUTION CODE

13. ABSTRACT (Maximum 200 Words)

The epothilones are 16-membered macrolides isolated from the myxobacteria, *Sorangium cellulosum*. Their mode of action is microtubule hyperstabilization, which is shared with the anticancer drug paclitaxel. The epothilones have been the subject of synthetic and biological studies and this has resulted in clinical trials for several epothilone derivatives. In order to learn more about the epothilone binding site on tubulin we have targeted the synthesis of epothilone affinity probes.

We have carried out tubulin labeling studies with two 12-hydroxylmethyl-derived arylazido epothilone analogues, however, no photoincorporation was observed. Studies toward the synthesis of an 8-hydroxymethyl analogue and a 4-hydroxyethyl epothilone derivative are at advanced stages of synthesis and will become available shortly for labeling studies. The chemistry procedures to obtain the various building blocks for the synthesis of the analogues has been validated, their synthesis has been scaled up, and the convergent assembly of the targeted molecules is underway.

14. SUBJECT TERMS
Multi-drug resistant breast cancer, epothilones, photoaffinity labels, tubulin

15. NUMBER OF PAGES
23

16. PRICE CODE

17. SECURITY CLASSIFICATION OF REPORT	18. SECURITY CLASSIFICATION OF THIS PAGE	19. SECURITY CLASSIFICATION OF ABSTRACT	20. LIMITATION OF ABSTRACT
Unclassified	Unclassified	Unclassified	Unlimited

NSN 7540-01-280-5500

Standard Form 298 (Rev. 2-89)
Prescribed by ANSI Std. Z39-18
298-102

Table of Contents

Introduction

The epothilones are novel 16-member macrolides (Figure 1) originally isolated from *Sorangium cellulosum,* a gram-negative myxobacteria.[1] They have an excellent biological profile against cancer cells, including multi-drug resistant cell lines. They also have proven effective at reducing tumor xenografts in vivo.[2] Many syntheses were completed for the epothilones and numerous analogues were made and tested for biological activity.[3] The results of this work have led to phase II clinical trials of epothilone B, phase II clinical trials for 15-azaepothilone B, phase I clinical trials for 21-aminoepothilone B and phase I clinical trials for epothilones.[3] In order to better understand the mechanism of action for the epothilones, microtubule hyperstabilization, we plan to study their binding site on tubulin. We have designed a synthesis of the epothilones that is amenable to the formation of hydroxymethyl substituents at various positions, which can be acylated with compounds that can covalently interact with tubulin (Figure 2). Through a combination of photoaffinity labeling, and radiolabeling experiments, we hope to determine the specific amino acids on tubulin that the epothilones are interacting with. This data can be used to design more selective analogues for cancer chemotherapy.

Body

In the second year of study we had reported the synthesis and the initial testing of the epothilone affinity analogues shown in Figure 3. The two arylazide analogues were found to be as active as epothilone B in a tubulin assembly assay and were therefore considered very promising probes to map the epothilone binding site on tubulin. In year three, the two new epothilone analogues were examined in photolabeling studies in the laboratory of our collaborator Professor Himes. However, none of the photoaffinity probes labeled tubulin. We have therefore concluded that the affinity labels at C12 are most likely located outside the epothilone binding pocket on tubulin and therefore unable to label tubulin.

Because of the negative results with the C12 derivatives we focused next on the synthesis of the C8, and C4 hydroxymethyl analogues of epothilones (Figure 2) for the attachment of photoaffinity probes.

Scheme 1 shows the general synthetic strategy that we have developed for the synthesis of epothilone photoaffinity analogues (see annual reports year 1 and 2). For the synthesis of the C8 hydroxymethyl analogue building block **B** needs to be modified (R = OH) and for the synthesis of the C4 analogues, one of the C4 methyl substituents of building block **A** will be converted to a hydroxymethyl group (R = OH) or a higher homologue.

Both approaches will use building block **C** (vinyl iodide). While we have prepared this building block before (Scheme 2 and reports of year 1 and 2), we needed to prepare it again on

large scale for the synthesis of the targeted affinity probes. We were able to improve the yield in the last step of the synthesis (Wittig reaction) from 55% to 73% by using HMPA as a co-solvent.

Synthesis of C8 modified analogues: For the synthesis of the C8 analogues we also needed to prepare building block **A** again (Scheme 3 and reports of year 1 and 2) on large scale.

For the synthesis of building block **B** (R = OH) we employed Evans chiral oxazolidinone to set the C8 stereochemistry (Scheme 4). (4*S*,5*R*)-(+)-4-Methyl-5-phenyl-2-oxazolidinone was acylated using 4-pentenoyl chloride in 88% yield. The subsequent alkylation was completed using titanium tetrachloride and benzoyloxymethyl chloride in 82% yield. Removal of the auxiliary using $LiBH_4$ provided the desired alcohol in 78% yield and allowed for facile recovery of the auxiliary. This route became the preferred one for the synthesis of the **B** fragment. The auxiliary was made economically from (1*S*,2*R*)-(+)-norephedrine and recycled after the reductive removal of the alcohol with $LiBH_4$. These features make this reaction pathway highly amenable to large scale.

Suzuki Reaction between vinyl iodide **C** and fragment **B** alkylborane provided the C7-C20 open chain fragment in 90% yield (Scheme 5). Straightforward functional group manipulation converted the primary OTBS into aldehyde **5.1** to set the stage for the diastereoselective aldol reaction. The next step was to join the C1-C6 ketone **A** with the C7-C20 aldehyde **5.1** (Scheme 6). Aldol reaction provided the C1-C20 fragment with a 10:1 ratio of the desired diastereoisomer which was protected as its TBS ether (Scheme 6). The primary TBS was then selectively removed using 40% HF/glass splinters in acetonitrile/diethyl ether. The alcohol **6.1** was oxidized to the corresponding acid (Scheme 7) in two steps: Dess-Martin oxidation followed by $NaClO_2$. Next, the C15 alcohol was selectively deprotected with TBAF and Yamaguchi macrolactonization ring closure provide the macrolactone. The secondary TBS groups were then removed using TFA to provide the diol **7.1**. All efforts to remove the benzyl protecting group from **7.1** failed to yield the targeted triol.

The 8-benzyloxymethyl epothilone derivative **7.1** was evaluated in a tubulin assembly assay and was found to posses no activity. This indicates that the C8 site of the epothilones may not be able to tolerate structural modifications.

Nevertheless, we decided to prepare the originally targeted 8-hydroxymethyl epothilone derivative by using a more easily removable hydroxyl protecting group, the TBDPS group (Scheme 8). As shown in Scheme 8, deprotection of the benzyl group using boron trichloride, followed by protection of the hydroxyl group in the form of a TBDPS ether (**8.1**) and removal of the chiral auxiliary, afforded the corresponding alcohol, which was oxidized to aldehyde **B**. After Suzuki coupling of fragment **8.1** and vinyl iodide **C**, the reaction product was reduced and oxidized to the corresponding aldehyde. Aldol reaction between the aldehyde and ketone **A**, followed by

desilylation provided intermediate **9.1** (9:1 ratio of diastereoisomers). This intermediate will be converted to the targeted 8-hydroxymethylepothilone using the chemistry shown in Scheme 7. Our second strategy to the targeted molecule is shown in Scheme 10. In this approach, aldol reaction between ketone **A** and aldehyde **B** provided the reaction product with excellent diastereoselectivity (> 95:5). The newly formed hydroxyl group was protected as silyl ether to form **10.1**. The next step that will be investigated is the Suzuki coupling between building blocks **10.1** and **C** to form **9.1**. Depending on the outcome of this reaction, we will use this approach (Scheme 10) or the strategy shown in Scheme 9 to complete the synthesis of the target compound. After completion of the synthesis, we plan to attach the photoprobes shown in Figure 3 to the 8-hydroxymethyl group of the epothilone derivative.

Synthesis of C4-modified analogues: We have made progress towards this goal as well. As mentioned before, we have scaled up the synthesis of building block **C** and also have sufficient quantities of building block **B** in hand. For the synthesis of the necessary building block **A** we need to introduce a C4-hydroxymethyl group. As shown in Scheme 11, Noyori reduction provided the optically active β-hydroxy ester. Frater alkylation[4] with benzyloxymethyl chloride gave very low yields. Therefore, the alkylation was carried out with trityloxyethyl chloride in moderate yield. The second Frater alkylation with methyl iodide resulted mostly in the formation of the O-alkylated product rather than forming the desired C-alkylated analogue. In a second approach (Scheme 12), we carried out the first alkylation with allyl iodide, followed by methylation and ozonolysis. This approach is very promising and should provide us with the desired building block **A** (R =CH_2OH) following the chemistry shown in Scheme 3.

Novel approach to the synthesis of the C12-C20 fragment: Due to reproducibility problem with the enantioselectivity of the CBS reduction (Scheme 2) on large scale, we attempted to synthesize the C12-C20 fragment using a different route. In our first attempt, we explored the Noyori reduction of β-ketoesters using ruthenium chiral catalysts (Table 1).[5] The reaction proceeded smoothly to give a 47% yield of the thiazole β-hydroxyester in 80% enantiomeric excess (entry 1). The enantioselectivity could be slightly enhanced by using the ethyl ester instead of the methyl ester. We applied this reaction to several γ,δ-unsaturated-β-ketoesters (Table 2). Most of these reactions provided the corresponding β-hydroxyesters in good yield and enantioselectivity. The best results were obtained for the fluorobenzene substrate, which proceeded in 88% yield and 94%ee. To further enhance the enantioselectivity, we replaced the BINAP ligand with other chiral ligands (Table 2), however, no enhancement of enantioselectivity was observed with these catalysts (entries 2 and 3).[6,7] Table 3 demonstrates that the presence of the γ-methyl group is important to retain the double bond in the substrate during reduction. Deletion of the methyl group yielded the over-reduced reaction products alongside the desired reaction products.

Key Research Accomplishments

- Scale up of common building blocks for the synthesis of the 8-hydroxymethyl analogue and the 4-hydroxymethyl analogue.
- Total synthesis of 8-benzyloxymethylepothilone A.
- Progress made towards the synthesis of the 8-hydroxymethyl epothilone analogue.
- Progress made towards the synthesis of a 4-hydroxymethyl analogue: Construction of the asymmetric quarternary carbon for the synthesis of C4 hydroxymethyl analogue.
- Developed enantioselective synthesis of γ,δ-unsaturated-β-hydroxy esters using the Noyori reduction for the large scale synthesis of building block **C**.

Reportable Outcomes

1. Michaelis, M. L.; Chen, Y.; Hill, S.; Reiff, E.; Georg, G. I.; Rice, A.; Audus, K. Amyloid Peptide Toxicity and Microtubule-Stabilizing Drugs. *J. Mol. Neurosci.* **2002**, *19*, 101.

2. Selective Reduction of γ,δ-Unsaturated β-Keto Esters to the Corresponding γ,δ-Unsaturated β-Hydroxy Esters; E. A. Reiff, B. S. N Reddy, J. Inagaki, J. Greiner and G. I. Georg; Abstracts of Papers, 37th Midwest Regional Meeting of the American Chemical Society, Lawrence, KS, Oct. 23-25, **2002**.

3. Synthesis of Epothilones A and B: Stereoselective Synthesis of Fragments; J.F. Greiner, E. A. Reiff, S. K. Nair, B. S. N. Reddy, R. Chakrasali, J.T. Henri and G. I. Georg; 40th Annual MIKI Meeting, University of Illinois, Chicago, April 12-13, **2002**.

4. G. I. Georg, B. S. N Reddy, E. A. Reiff, J. Inagaki, J. Greiner and R. H. Himes; Total synthesis of 25-hydroxyepothilone C. Abstracts of Papers, 225th ACS National Meeting, New Orleans, LA, United States, March 23-27, 2003, MEDI-120.

5. G.I. Georg, E. R. Reiff, S. Nair, A. R. Tunoori, J. Henri; Synthesis of epothilones. US Patent 6,457,303 issued.

6. Ph.D. degree Emily Reiff, University of Kansas 2002 (see last report). Current employment: Bristol Myers Squibb, oncology division, development of epothilones as anticancer agents.

Conclusions: The preparation of the building blocks for the synthesis of the target molecules has been largely accomplished. Improvements in their synthesis have been made and their synthesis has been scaled up. The synthesis of the 8-hydroxymethyl epothilone analogue is well under way and will be completed shortly. The 4-hydroxymethyl analogue should be available soon as well. Both epothilone analogues will be acylated with the photoaffinity probes shown in Figure 3 and then evaluated for their ability to photolabel tubulin in the laboratory of our collaborator.

References

(1) Höfle, G.; Bedorf, N.; Gerth, K.; Reichenbach, H. *Offenlegungsschrift der Bundesrepublik Deutschland* **1993**, DE 4138042 A1.
(2) Chou, T. C.; O'Connor, O. A.; Tong, W. P.; Guan, Y.; Zhang, Z. G.; Stachel, S. J.; Lee, C.; Danishefsky, S. J. *Proc. Natl. Acad. Sci. U.S.A.*, *98*, 8113-8118.
(3) *Anticancer Agents: Frontiers in Cancer Chemotherapy*; Ojima, I.; Vite, G. D.; Altman, K.-H., Eds.; ACS: Washington, DC, 2001.
(4) Frater, G. *Helv. Chim. Acta* **1979**, *62*, 2825-2832.
(5) Noyori, R.; Ohkuma, T.; Kitamura, M.; Takaya, H.; Sayo, N.; Kumobayashi, H.; Akutagawa, S. *J. Am. Chem. Soc.* **1987**, *109*, 5856-5858.
(6) Zhou, Y.-G.; Tang, W.; Wang, W.-B.; Li, W.; Zhang, X. *J. Am. Chem. Soc.* **2002**, *124*, 4952-4953.
(7) Genet, J. P.; Ratovelomanana-Vidal, V.; Can de Andrade, M. C.; Pfister, X.; Guerreiro, P.; Lenoir, J. Y. *Tetrahedron Lett.* **1995**, *36*, 4801-4804.

Appendices

Figure 1. Structures of the epothilones.

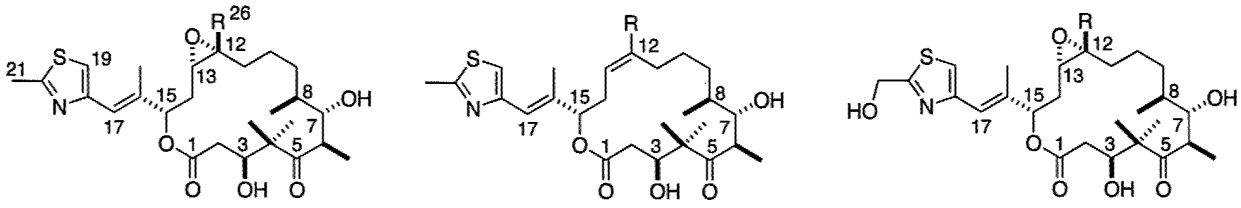

R = H, epothilone A (**1a**)
R = Me, epothilone B (**1b**)

R = H, epothilone C (**1c**)
R = Me, epothilone D (**1d**)

R = H, epothilone E (**1e**)
R = Me, epothilone F (**1f**)

Figure 2. Sites on the epothilone ring targeted for the attachment of photoaffinity labels.

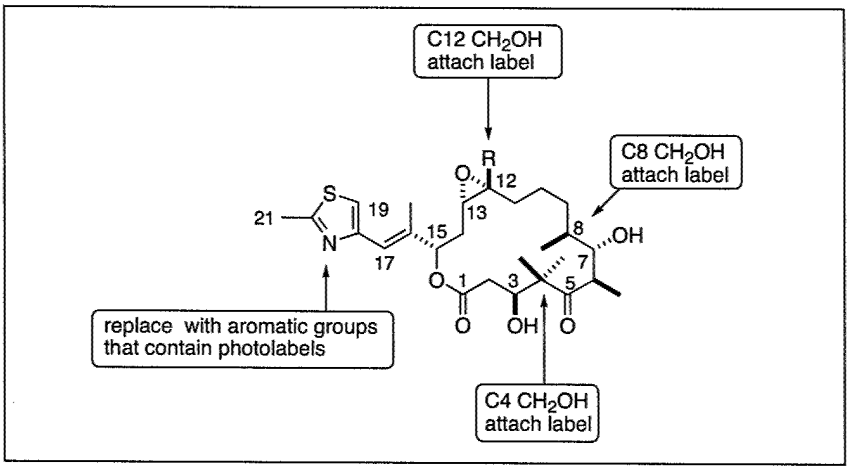

Figure 3. Synthesized C12 epothilone affinity analogues.

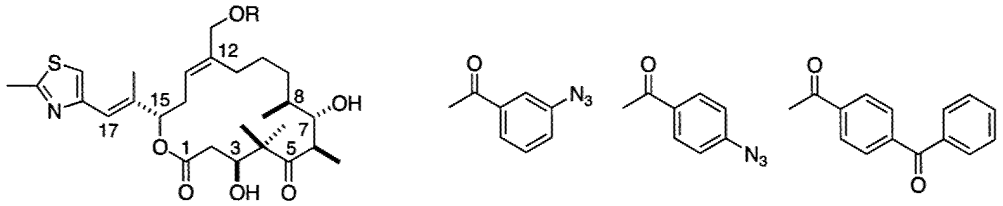

Scheme 1

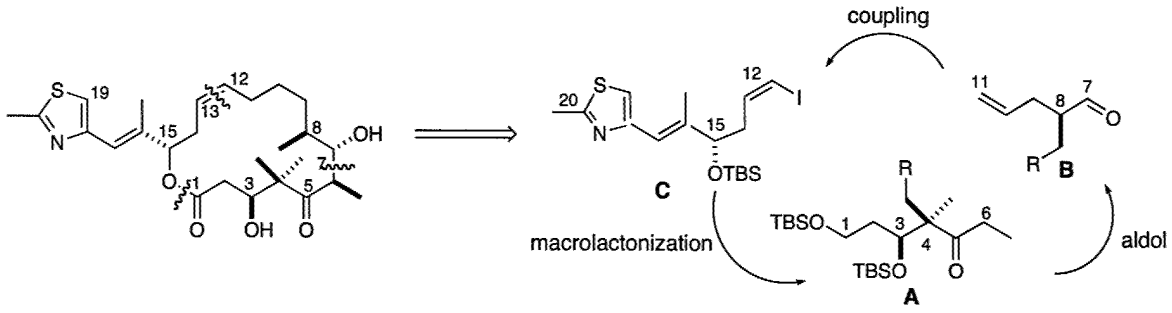

Scheme 2

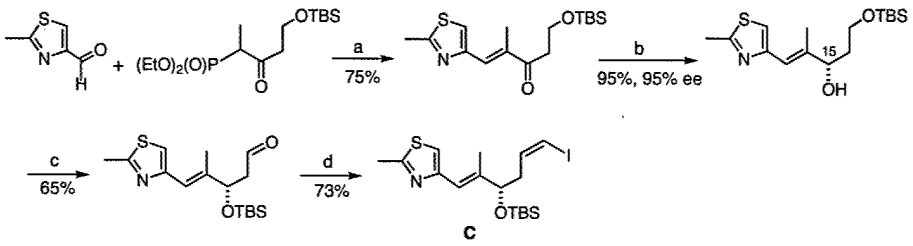

a) Ba(OH) x 2.8 H_2O, THF, THF: H_2O (40:1), b) (*R*)-2-Me-CBS-oxazaborolidine (0.5 eq), BH_3 xMe_2S (1.5 eq), CH_2Cl_2, 0 °C, 2 h, then ethanolamine, c) i) TBSOTf, 2,6-lutidine, CH_2Cl_2, -78 °C; ii) HF (48% aq.), glass splinters, MeCN:Et_2O (1:1), 0 °C; iii) Dess -Martin periodinane, CH_2Cl_2, d) PPh_3CH_2I, NaHMDS, THF, then HMPA at -78 °C, then aldehyde in THF, -78 °C -> rt.

Scheme 3

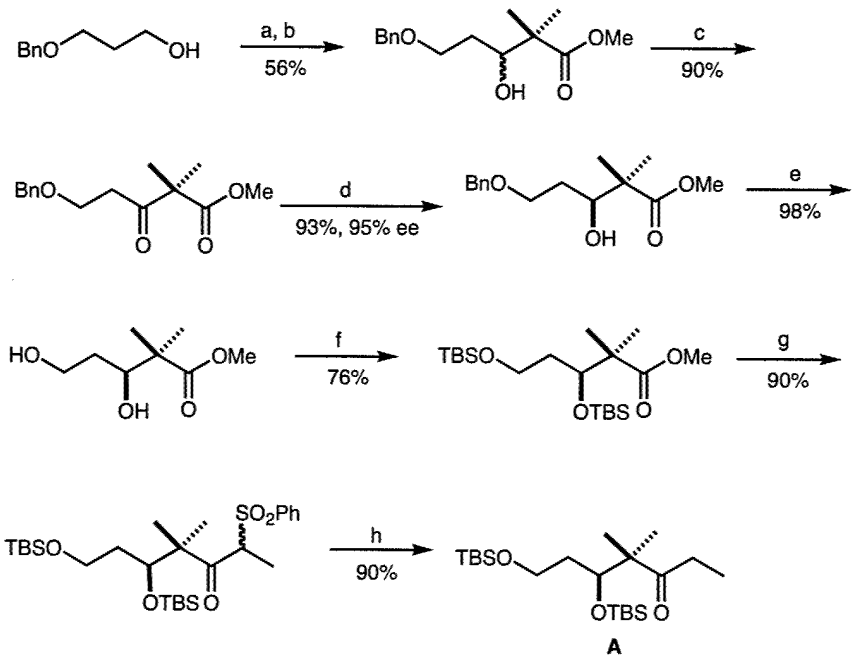

A

a) TEMPO/NaOCl, CH_2Cl_2, 0 °C, rt, b) methyl isobutyrate, diisopropylamine/n-BuLi, THF, -78 °C, c) PDC, molecular sieves, CH_2Cl_2, rt, d) $RuBr_2$(*S*)-binap, H_2, MeOH, 60 *psi*, 60°C, e) H_2, 10%Pd/C, 60*psi*, MeOH, f) TBSCl, Imidazole, DMAP, DMF, 100 °C, g) $PhSO_2Et$, *n*-BuLi, -78 °C, rt, h) Na(Hg), Na_2HPO_4, MeOH, rt

Scheme 4

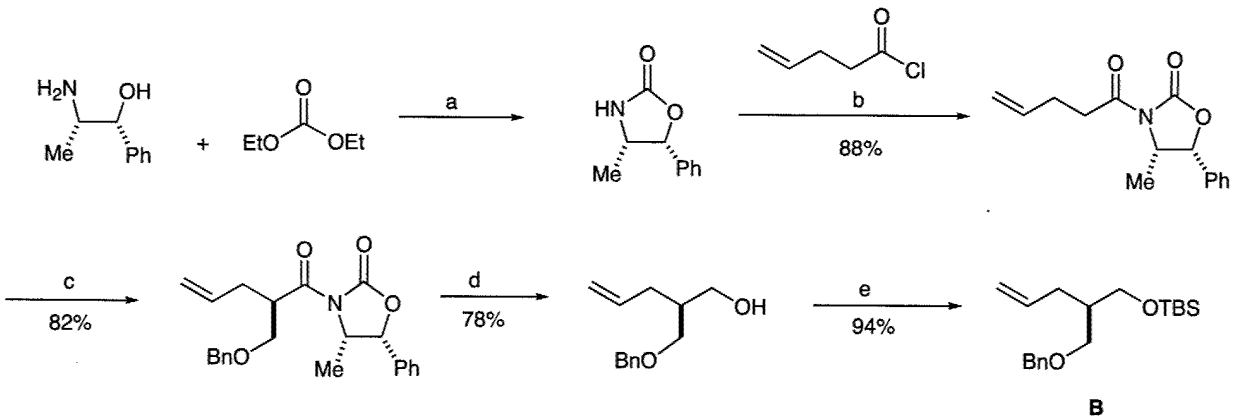

B

a) K_2CO_3, 140 °C, b) n-BuLi, -78 °C, THF, c) $TiCl_4$, DIEA, $BnOCH_2Cl$, 0 °C, CH_2Cl_2, d) $LiBH_4$, Et_2O:H_2O, e) TBSOTf, 2,6-lutidine.

Scheme 5

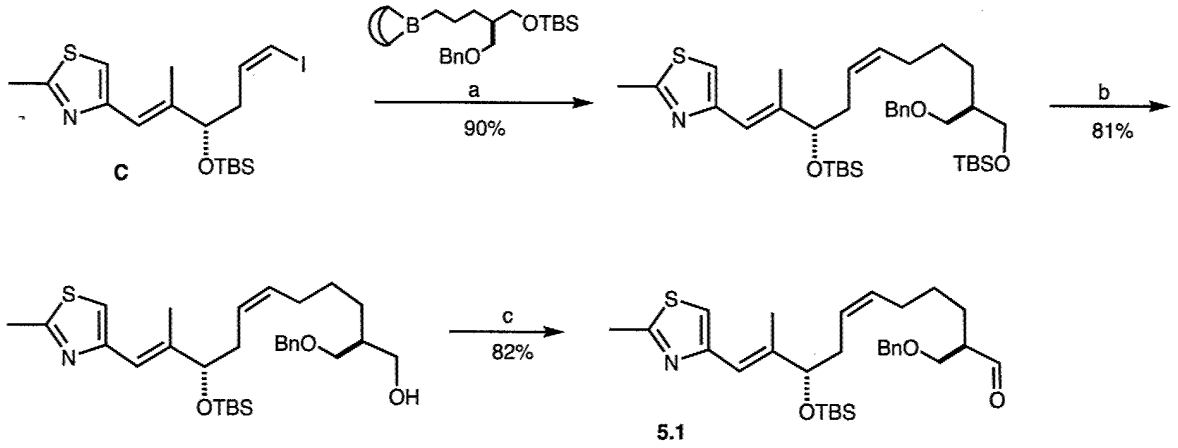

a) $PdCl_2(dppf)$, CH_2Cl_2, Ph_3PAs, $CsCO_3$, DMF, H_2O, rt, b) 40 % HF, H_2SF_6 (cat.), CH_3CN : Et_2O, 0 °C, c) Dess-Martin periodinane, CH_2Cl_2, rt.

Scheme 6

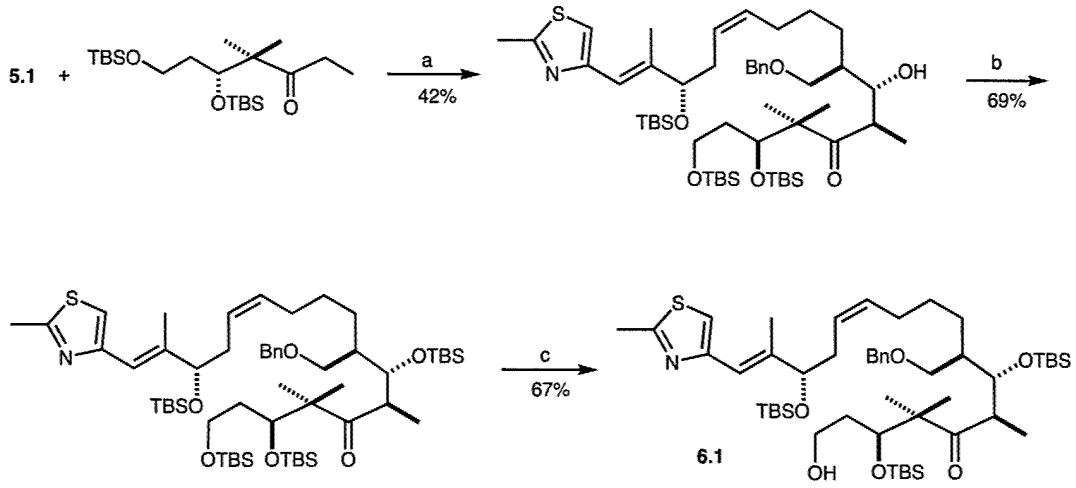

a) Disopropylamine, n-BuLi, -78 °C, rt, b) TBSOTf, 2,6-lutidine, CH_2Cl_2, c) 40% HF x H_2SiF_6 (cat.), CH_3CN:CH_2Cl_2.

Scheme 7

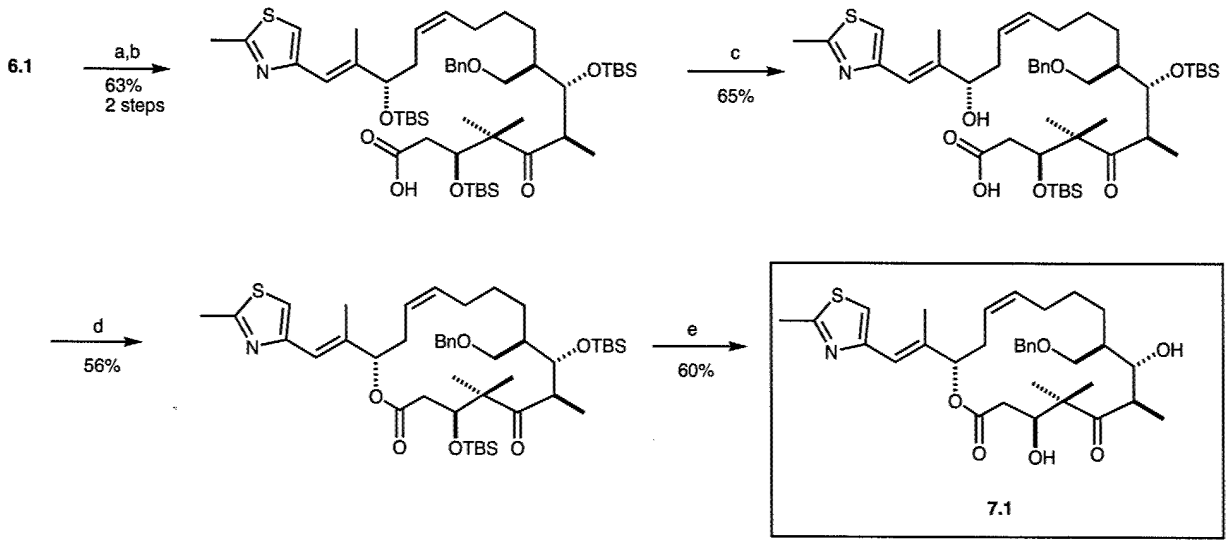

a) Dess-Martin periodinane, CH_2Cl_2, rt, b) $NaClO_2$, NaH_2PO_4, t-BuOH, H_2O, 2-methyl-2-butene, c) TBAF, THF, rt, d) 2,4,6-trichlorobenzoyl chloride, DMAP, Et_3N, THF, toluene, 70 °C, e) TFA 20% v/v in CH_2Cl_2, -20 °- 0 °C.

Scheme 8

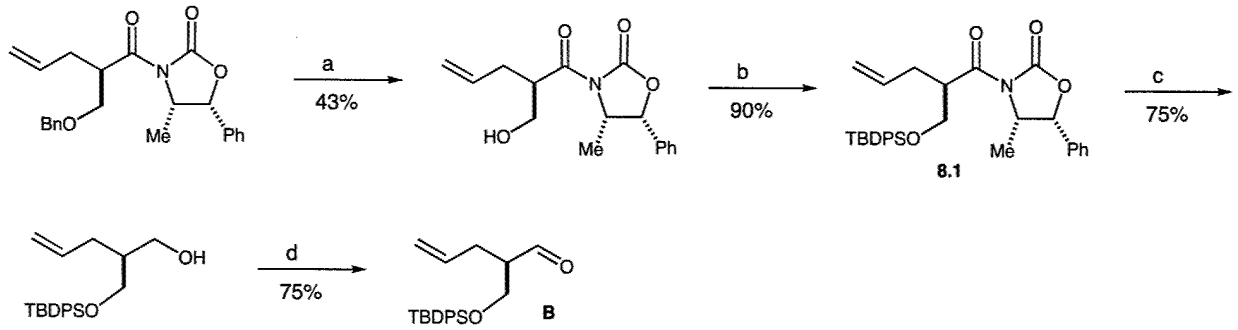

a) BCl_3, CH_2Cl_2, -78 °C, b) TBDPSCl, imidazole, DMF, 70 °C, d) Dess-Martin periodinane, CH_2Cl_2.

Scheme 9

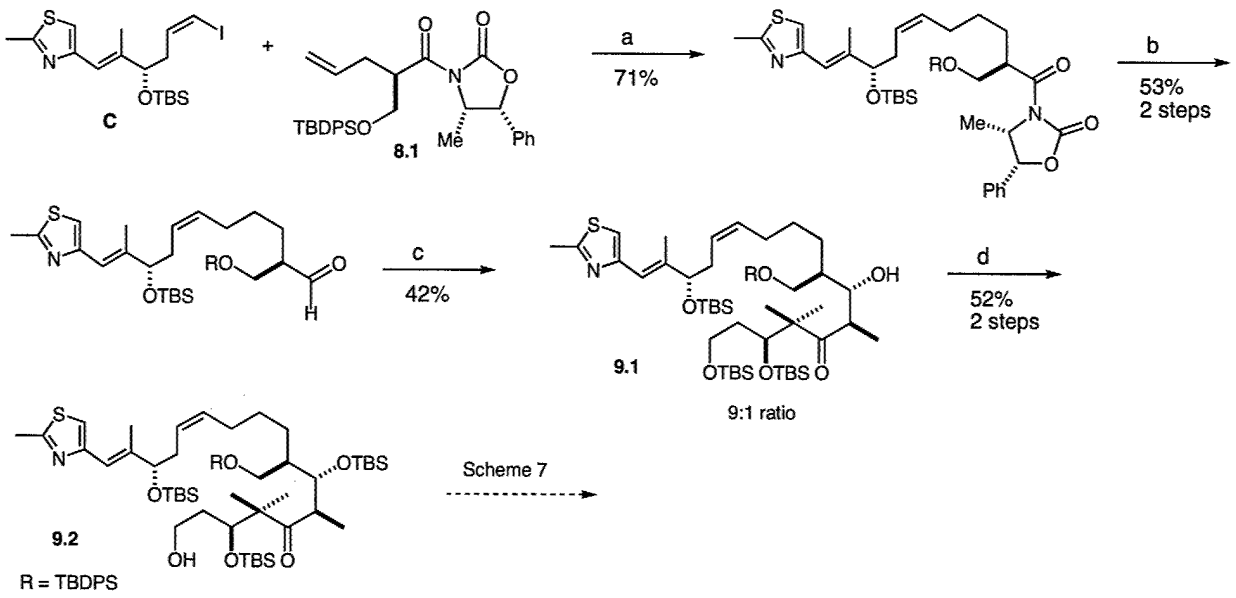

a) $PdCl_2(dppf)$ CH_2Cl_2, Ph_3As, $CsCO_3$, DMF, H_2O, b) i. $LiBH_4$, Et_2O, H_2O, 0 °C, ii. IBX, EtOAc, 70 °C, c) **A** (R = H), LDA, THF, -78 °C, d) i. TBSOTf, 2,6-lutidine, 0°C, CH_2Cl_2. ii. 40% HF / glass splinters, CH_3CN:Et_2O (1:1), 0 °C.

Scheme 10

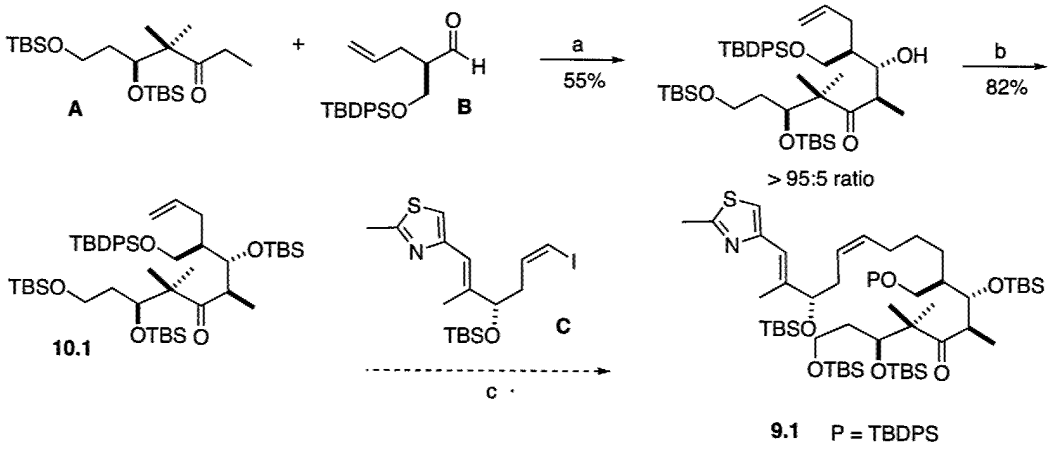

a) LDA, THF, -78 °C, b) TBSOTf, 2,6-lutidine, CH_2Cl_2, 0 °C, c) $PdCl_2(dppf)$ CH_2Cl_2, Ph_3As, $CsCO_3$, DMF, H_2O.

Scheme 11

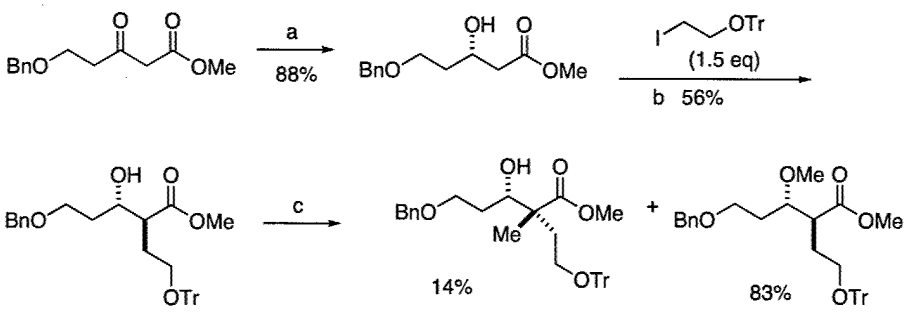

a) $RuBr_2$(*S*)-BINAP (0.5 mol%), H_2 (55 psi), MeOH, rt, 48 h, b) LDA (2.3 eq), HMPA (2.5 eq), THF, -78 °C to rt, c) LDA (2.5 eq), MeI (1.5 eq), HMPA (2.5 eq), THF, -78 °C to rt.

Scheme 12

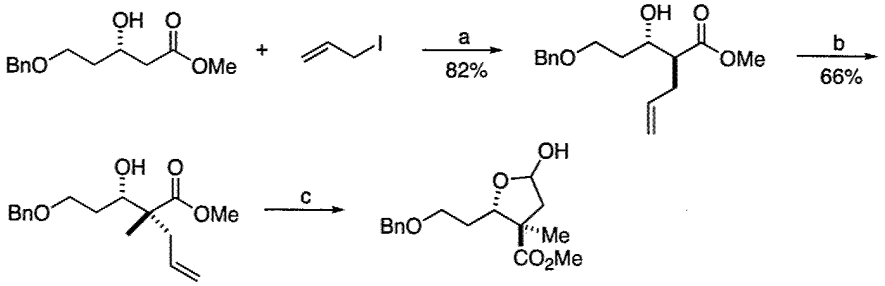

a) LDA (2.5 eq), HMPA (2.5 eq), THF, -78 to -20 °C, b) MeI (1.5 eq), LDA (2.5 eq), HMPA (2.5 eq), THF, -78 to -20 °C, c) O_3, then Me_2S, -78 °C.

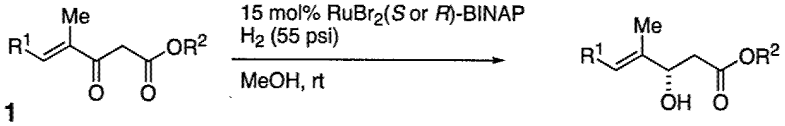

Table 1

entry	R^1	R^2	BINAP	time	yield	% ee[a]
1	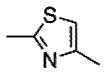	Me	(*R*)	3 h	47%	80
2	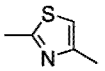	Et	(*S*)	2 h	50%	83
3		Me	(*S*)	5 h	89%	89
4		Et	(*S*)	3 h	79%	87
5		*t*Bu	(*S*)	5 h	82%	68
6	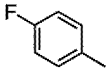	Me	(*R*)	3 h	86%	94
7	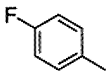	Et	(*S*)	3 h	84%	82
8	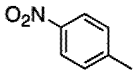	Et	(*S*)	3.5 h	85%	88
9	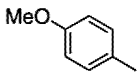	Et	(*S*)	2 h	81%	87
10	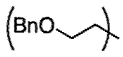	Et	(*S*)	3 h	68%	83
11		Et	(*S*)	2.5 h	65%	75

[a] The enantiomeric excess was determined by HPLC analysis (Chiralcel-OD-H)

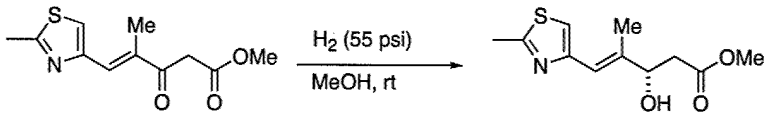

Table 2

entry	Catalyst	time	yield	% ee[a]
1	$RuBr_2$[(*R*)-BINAP], 15 mol%	3 h	47%	80
2	$RuBr_2$[(*R*)-TolBINAP], 15 mol%	3h	45%	80
3	$RuBr_2$[(*R*)-MeO-BIPHEP], 15 mol%	3 h	50%	82
4	$RuCl_2$[(*R*)-xylyl-*o*-BINAPO], 5 mol%	48 h	-[b]	–

[a] The enantiomeric excess was determined by HPLC analysis (Chiralcel-OD-H, hexane:*i*-propanol=9:1, 1mL/min, 14.9 min (major), 17.5 min (minor)
[b] This reaction did not proceed (S.M. was recovered).

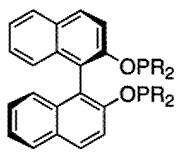

(*R*)-BINAP: R = C_6H_5

(*R*)-TolBINAP: R = 4-MeC_6H_4

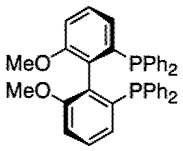

(*R*)-MeO-BIPHEP

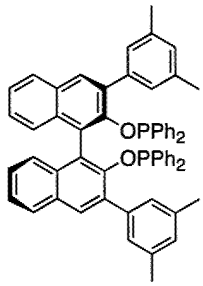

(*R*)-xylyl-*o*-BINAPO

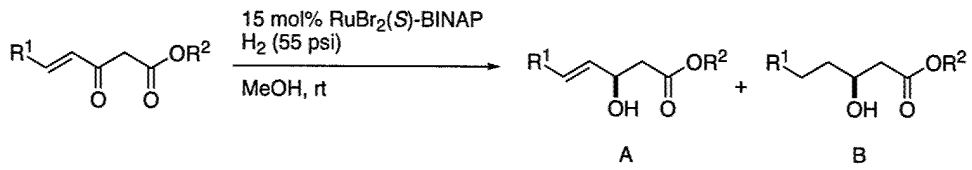

Table 3

entry	R	R^2	time	yield	A : B	% ee
1		Et	2 h	65%	1 : 1	-
2	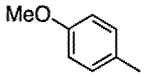	Et	2 h	72%	1 : 1	-
3	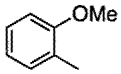	Et	2 h	70%	1 : 1	-
4	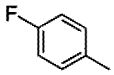	Et	2 h	75%	1 : 1	-
5	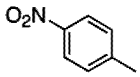	Et	2 h	69%	1 : 1	-

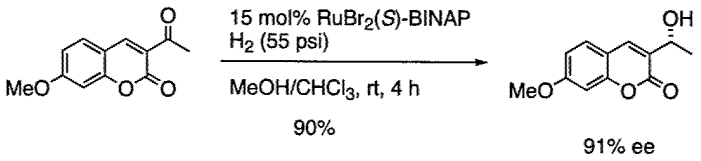

Journal of Molecular Neuroscience

ISSN0895-8696/02/19:101–105/$11.25

Amyloid Peptide Toxicity and Microtubule-Stabilizing Drugs

Mary L. Michaelis,[*,1] *Yingxue Chen,*[1] *Sarah Hill,*[1] *Emily Reiff,*[2] *Gunda Georg,*[2] *Antonie Rice,*[3] *and Kenneth Audus*[3]

[1]*Department of Pharmacology and Toxicology, University of Kansas, Malott Hall 5064, 1251 Wescoe Hall Drive, Lawrence, KS 66045;* [2]*Department of Medicinal Chemistry, University of Kansas, Malott Hall 4070, 1251 Wescoe Hall Drive, Lawrence, KS 66045; and* [3]*Department of Pharmaceutical Chemistry, University of Kansas, 108 MCRL, 2099 Constant Avenue, Lawrence, KS 66047*

Received October 2, 2001; Accepted October 16, 2001

Abstract

Based on microtubule (MT) disruption observed in primary neurons exposed to fibrillar amyloid peptides (Aβ), we tested the potential protective effect of MT-stabilizing drugs such as Taxol® against Aβ-induced disruption of the cytoskeleton. Although Taxol® was strongly protective, the fact that it does not cross the blood brain barrier (BBB) led us to synthesize and test other agents with MT-stabilizing properties and possible penetration into the brain. Our studies have thus far demonstrated that several MT-stabilizing agents, including some with structures quite different from that of Taxol®, showed significant protective effects. However, not all agents that promoted MT-assembly were protective, suggesting additional mechanisms are involved in the actions of the drugs. A small number of neuroprotective compounds appear to have potential to enter the brain and thus might be tested to see if they slow progression of neurodegeneration in an appropriate animal model of Alzheimer's disease.

Index entries: Microtubule-stabilizing drugs; Aβ toxicity; primary neurons; neurofibrillary pathology; blood brain barrier.

Introduction

Deposition of β-amyloid peptide (Aβ) and hyperphosphorylation of τ protein leading to neurofibrillary tangles (NFTs) are the neuropathological markers associated with neuronal dysfunction and cell death in Alzheimer's disease (AD). The crucial role of Aβ in the pathogenesis of AD is strongly supported by the genetics of abnormalities in the amyloid precursor protein (APP) (e.g., Mullan and Crawford, 1993) and the enhanced $A\beta_{1-42}$ formation and deposition in senile plaques in individuals with mutations in the presenilin genes (e.g., Scheuner et al., 1996). In addition, both in vivo and in vitro studies have shown that accumulation of fibrillar aggregates of Aβ can trigger neurodegenerative changes (e.g., Yankner, 1996; Mattson, 1997). The role of NFTs in neurodegeneration was less certain prior to the discovery that mutations in the gene encoding the τ protein were associated with neurodegnerative diseases linked to chromosome 17 (Hutton et al., 1998; Spillantini et al., 1998; Goedert et al., 1999; Sergeant et al., 1999). The neurofibrillary degeneration observed in the 'tauopathies' strongly indicates that τ dysfunction leads to neuronal cell death. *Tau* is a microtubule (MT)-associated protein that binds to and stabilizes the MT network in cells, and excess phosphorylation of τ on specific serine/threonine residues leads to self-assembly of τ proteins and failure to regulate the dynamic instability essential for MTs to function normally. Although several studies had reported that deposition of Aβ in the vicinity of neurons enhanced τ phosphorylation in in vitro neuronal cell cultures (e.g., Busiglio et al., 1995; Le et al.,

*Author to whom all correspondence and reprint requests should be addressed. E-mail: mlm@ukans.edu

1997), and in vivo when Aβ is deposited in the brain (Sigurdsson et al., 1996; Geula et al., 1998), a link between the two lesions in AD was not widely accepted. However, two recent papers reported that transgenic mice expressing the mutant form of human τ (P301L) showed very significant enhancement in neurofibrillary pathology when the mice also expressed a mutated APP (Lewis et al., 2001) or when Aβ fibrils were injected into the brain (Gotz et al., 2001). These observations indicate significant interactions between Aβ deposits and NFTs in the degenerative cascades in AD brain and suggest that drugs targeted to preventing neurofibrillary pathology may help slow the progression of the neurodegeneration.

Based on the pronounced disruption of MT integrity observed when primary neurons in culture are exposed to fibrillar Aβ, we have been testing the hypothesis advanced by Lee et al., (1994) that Taxol® and analogs with MT-stabilizing properties might protect neurons against Aβ-induced disruption of the cytoskeleton. We previously reported that Taxol does protect primary neurons against the toxicity induced by Aβ (Michaelis et al., 1998). However, because Taxol does not cross the blood-brain barrier (BBB), we have been synthesizing and testing various other agents with MT-stabilizing properties. The goal of these experiments is to determine if: 1) structurally diverse drugs that promote MT assembly also protect neurons against Aβ, 2) MT-stabilizing activity alone is sufficient to protect the neurons, and 3) agents can be identified that both protect neurons against Aβ toxicity and cross the BBB. Our studies have thus far demonstrated that several MT-stabilizing agents, including some with structures quite different from that of Taxol, showed significant protective effects. However, not all agents that promoted MT-assembly were protective, suggesting that additional mechanisms are involved in the actions of the drugs. A small number of compounds did protect neurons against Aβ toxicity and have potential to enter the brain.

Methods

Primary neuronal cultures were prepared from brains of embryonic d 18 rats as described previously (Michaelis et al., 1998). The small toxic $A\beta_{25-35}$ was synthesized in the University's Biochemical Research Lab, and the larger $A\beta_{1-42}$ was obtained from Bachem. Both peptides were prepared as described and added directly to the culture medium, usually at 10 μ*M* final concentration (Michaelis et al., 1998). Taxol was obtained from Dabur, India, Ltd., and Taxotere from Rhone-Poulenc Rohrer, Inc., France. The UK100 was a gift from Schering AG, Berlin, and GS164 was synthesized as described (Shintani et al., 1997). All MT-stabilizing agents were prepared as 2.5 m*M* stocks in dimethylsulfoxide (DMSO). Control cultures received the DMSO vehicle alone, and the final concentration of DMSO never exceeded 0.04%. Assays were carried out at 48 h following Aβ peptide addition.

Measurement of Cell Viability

Effects of the Aβ peptides and the MT-stabilizing drugs were primarily determined by monitoring neuronal cell survival using the Live/Dead assay as previously described (Michaelis et al., 1998). After incubation with calcein and propidium iodide, the dishes were rinsed and placed on a Nikon inverted microscope with epifluorescence. Digital images were captured and saved in Adobe Photoshop™. Scoring of viable neurons was performed in 6–12 microscopic fields per culture dish in duplicate dishes for each treatment, using at least 2 separate embryonic culture preparations. Induction of apoptosis during exposure of the neurons to Aβ was monitored using an *in situ* assay for capase activation, CaspACE™ FITC-VAD-FMK (Promega Corp., Madison, WI). The fluorescent caspase inhibitor is cell-permeable and irreversibly binds to activated caspases, allowing for detection of the apoptotic cascade in intact cells. A phase-contrast image of each field of neurons was captured using DIC optics and the same field was captured under fluorescence. The 2 images were superimposed and the percentage of the total cell population that was fluorescent and thus undergoing apoptosis was determined by direct cell counting. Multiple fields were analyzed for each treatment condition as described in the Live/Dead assay, and data were expressed as the percent of apoptotic cells.

Determination of Permeability of MT-Stabilizing Agents into the Brain

Primary cultures of brain microvessel endothelial cells (BMECs) were used as a model to evaluate potential permeation into the brain for newly synthesized agents (Rose and Audus, 1998). Transcellular diffusion/transport experiments were done with horizontal side-by-side diffusion chambers with confluent monolayers as described (Audus et al., 1996). The 'donor' chamber was pulsed with the drug and its permeation determined by sampling the 'receiver' chamber at various time points, using

high-pressure liquid chromatography (HPLC) techniques or liquid scintillation counting to detect the presence of the drug.

Results

Our initial studies revealed a dramatic enhancement in survival of neurons in cultures that received Taxol 2 h before addition of Aβ, compared to cultures treated with Aβ only (Michaelis et al., 1998). Our next goal was to determine if other agents with demonstrated MT-stabilizing activity also protected neurons against Aβ toxicity. Several Taxol analogs, as well as structurally diverse compounds with MT-assembly activity comparable to that of Taxol, were tested first to see if the drugs alone produced toxicity and, secondly, to see if addition of the drugs blocked Aβ-induced cell death. Figure 1 shows results obtained with a small sample of the agents that have been tested. Approximately 83% of the neurons were viable in control cultures but, in the presence of 10 μ*M* $A\beta_{25\text{-}35}$, the percentage of surviving neurons was reduced to slightly more than 50% within 48 h (Fig. 1). With the possible exception of Taxotere, addition of several different MT-stabilizing drugs alone for 48 h produced no neuronal cell death as shown by the open bars. When each of the MT-stabilizing agents was added at the indicated concentrations 2 h prior to addition of Aβ, all of the cultures showed a statistically significant increase in neuronal survival compared to cultures exposed to peptide alone. The percentage of surviving neurons in the Aβ plus drug-treated cultures was very close to 80%, with Taxol and Tx67 showing the strongest protection and no detectable drug-induced toxicity. It is important to point out that we have obtained essentially similar results when the larger $A\beta_{1\text{-}42}$ peptide was tested with a more limited set of MT-stabilizing agents. We have also carried out parallel experiments using an *in situ* marker of apoptosis, i.e., caspase activation, and found that ~ 33% of neurons exposed to Aβ were apoptotic compared to ~ 7% in control cultures. Pretreatment with Taxol before addition of Aβ reduced the apoptotic cells to less than 10% of all the neurons, suggesting that the drug was preventing the apoptotic cascade initiated by Aβ in some neurons. Cultures treated with Taxol alone did not differ at all from the controls.

Taxotere and Tx67 are close structural analogs of Taxol, but UK100 and GS 164 are very different compounds. The potency of UK100 in a MT-assembly assay was fairly similar to that of Taxol, but GS 164 was considerably less potent. This may explain why

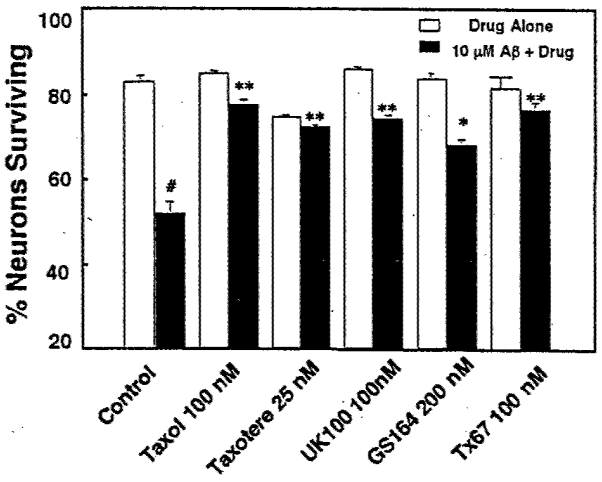

Fig. 1. Effects of MT-stabilizing drugs on Aβ-induced cell death in primary neurons. Cells were treated with indicated concentrations of the drug only or the drug 2 h before addition of 10 μ*M* $A\beta_{25\text{-}35}$ and analyzed 48 h later with the Live/Dead assay. Data are presented as the mean percentage (±s.e.m.) of live neurons. Approx ~1500 neurons per treatment were analyzed. The Aβ only cultures differed significantly from neurons exposed to all other conditions (#$p < 0.001$). Cultures exposed to the MT-stabilizing agents 2 h before Aβ treatment all differed significantly from Aβ only cultures as indicated: *$p < 0.05$, **$p < 0.001$.

GS 164 at a concentration of 200 nM was still not quite as effective as UK 100 or the Taxol analogs. Taxotere is considerably more potent than Taxol in stabilizing MTs, and the concentration of this drug that provided maximal protection was 25 n*M*. At concentrations greater than 25 n*M*, Taxotere alone produced significant toxicity. Confocal images of neurons exposed to higher concentrations of Taxotere revealed thick neuritic processes, suggesting that this agent was causing substantial MT bundling and loss of MT dynamics required for normal cellular functions.

In efforts to identify MT-stabilizing agents with potential to enter the brain, we synthesized and tested a large array of drugs. Although we hypothesized that agents with MT-stabilizing activity similar to that of Taxol would protect neurons against Aβ, we found that some agents did not show this activity. Tests with rapidly dividing cells indicated that this was not due to failure of the compounds to enter the cells. At this point in time, it appears that MT-stabilization alone is not sufficient and that the protection against Aβ requires the drugs to produce some additional cellular effects. Given recent observations that Taxol influences signal-transduction events in various types of cells (e.g., Blagosklonny

Table 1

Compounds	Permeability cm^2/s
^{3}[H] Taxol	2.98 E –6
TX67	4.50 E –4
7-Succinate Taxol	3.14 E –4
DH-1	2.34 E –4
DH-2	1.40 E –3
DH-3	7.27 E –4
DH-4	6.07 E –4
YBL-2176-10G	5.69 E –5
YBL-2176-G	2.72 E –4
YBL-2176-S	2.51 E –4
YBL-2172	2.50 E –4
^{14}[C] Sucrose	7.52 E –5
^{14}[C] Mannitol	3.98 E –4

and Fojo, 1999), it seems plausible the effective MT-stabilizing drugs might be acting through more than one mechanism.

Our evaluation of MT-stabilizing agents involves not only protection against Aβ toxicity but also likely permeation through the BBB. Table 1 shows permeability coefficients of some of the MT-stabilizing agents tested in the diffusion chamber with the BMECs. Clearly the DH series of agents exhibited the greatest permeability through the BMEC monolayers, with DH-2 being 3 orders of magnitude more likely to cross the BBB than Taxol. However, somewhat surprisingly, this series of agents exhibited essentially no neuroprotective effects when tested in the Aβ toxicity assay with neurons. The next most promising agent for entry into the CNS is Tx67 and, as shown in Fig. 1, this agent has excellent neuroprotective activity.

Discussion

Our results indicate that drugs with MT-stabilizing activity can protect neurons against the toxic cascade initiated by Aβ in an in vitro model system. However, it appears that MT stabilization alone is not sufficient, and the drugs must produce some additional cellular effects to be protective. We are examining the influence of these agents on the phosphorylation state of τ as one possible site of action. Although we synthesized a large library of Taxol analogs using combinatorial chemistry, not all agents promoted MT assembly and thus were not tested in the cell assays. Of the Taxol-like agents tested, Tx67 was the most promising in terms of exhibiting both neuroprotective properties and potential to cross the BBB. Consequently we are testing this agent in intact mice to see, first, if it actually reaches the brain following peripheral administration and, secondly, if chronic treatment with the drug alone produces any observable toxicity in the brain tissue. If the results of these studies are positive, we plan to test the compound in some of the transgenic mouse models for AD pathology.

The strong evidence implicating Aβ as the primary culprit in the pathogenesis of AD has made this peptide the major focus of efforts to develop therapeutic interventions. Inhibition of the secretases, immune-mediated clearance of Aβ, and inactivation of the free-radical-inducing properties of the peptide are certainly promising avenues for minimizing or possibly eliminating the early events that lead to neuronal cell death. Nevertheless, each of these strategies still faces many caveats. Recent studies suggesting a strong link between Aβ deposition and NFTs lend support to the assertion that slowing the progression of AD may ultimately require attacks on multiple targets in the neurodegenerative cascade. Our observations with MT-interacting drugs indicate that agents targeted to more downstream events such as Aβ-induced loss of cytoskeletal integrity also have the potential to enhance cell survival, even as the toxic peptide is being deposited in the brain. We are looking forward to the opportunity to test these agents in AD mouse models that exhibit clear neurodegenerative changes.

Acknowledgments

This work was supported by the Inez Jay Fund, University of Kansas, and the Institute for the Study of Aging, Inc., New York.

References

Audus K. L., Ng L., Wang W., and Borchardt R. T. (1996) Brain microvessel endothelial cell culture systems. *Pharmaceut. Biotechnol.* **8**, 239–258.

Blagosklonny M. V. and Fojo T. (1999) Molecular effects of paclitaxel: myths and reality. *Int. J. Cancer* **83**, 151–156.

Busciglio J., Lorenzo A., Yeh J., and Yanker B. A. (1995) β-Amyloid fibrils induce tau phosphorylation and loss of microtubule binding. *Neuron* **14**, 879–888.

Geula C., Wu C. K., Saroff D., Lorenzo A., Yuan M., and Yankner B. A. (1998) Aging renders the brain vulnerable to amyloid beta-protein neurotoxicity. *Nature Med.* **4**, 827–831.

Goedert M., Spillantini M. G., Crowther R. A., et al. (1999) Tau gene mutation in familial progressive subcortical gliosis. *Nature Med.* **5**, 454–457.

Gotz J., Chen F., Dorpe J., and Nitsch R. M. (2001) Formation of neurofibrillary tangles in P301L Tau trans-

genic mice induced by Aβ42 fibrils. *Science* **293**, 1491–1495.

Hutton M., Lendon C. L., Rizzu P., Baker M., et al. (1998) Association of missense and 5′-splice-site mutations in tau with the inherited dementia FTDP-17. *Nature* **393**, 702–705.

Le W., Xie W. J., Kong R., and Appel S. H. (1997) β-Amyloid-induced neurotoxocity of a hybrid septal cell line associated with increased Tau phosphorylation and expression of β-amyloid precursor protein. *J. Neurochem.* **69**, 978–985.

Lee V. M. Y., Daughenbaugh R., and Trojanowski J. Q. (1994) Microtubule stabilizing drugs for the treatment of Alzheimers-Disease. *Neurobiol. Aging* **15**, **Suppl.** S87–S89.

Lewis J., Dickson D. W., Lin, W. L., Chisolm L., et al. (2001) Enhanced neurofibrillary degeneration in transgenic mice expressing mutant Tau and APP. *Science* **293**, 1487–1491.

Mattson M. P. (1997) Cellular actions of beta-amyloid precursor protein and its soluble and fibrillogenic derivatives. *Physiolog. Rev.* **77**, 1081–1132.

Michaelis M. L., Ranciat N., Chen Y., Bechtel M., Ragan R., Hepperle M., Liu Y., and Georg G. (1998) Protection against β-amyloid toxicity in primary neurons by paclitaxel (Taxol). *J. Neurochem.* **70**, 1623–1627.

Mullan M. and Crawford F. (1993) Genetic and molecular advances in Alzheimers-Disease. *Trends Neurosci.* **16**, 398–403.

Rose J. M. and Audus K. L. (1998) Receptor-mediated angiotensin II transcytosis by brain microvessel endothelial cells. *Peptides* **19**, 1023–1030.

Scheuner D., Eckman C., Jensen M., Song X., Citron M., et al. (1996) Secreted amyloid beta-protein similar to that in the senile plaques of Alzheimer's disease is increased in vivo by the presenilin 1 and 2 and APP mutations linked to familial Alzheimer's disease. *Nature Med.* **2**, 864–870.

Sergeant N., Wattez A., and Delacourte A. (1999) Neurofibrillary degeneration in progressive supranuclear palsy and corticobasal degeneration: Tau pathalogies with exclusively "Exon 10" isoforms. *J. Neurochem.* **72**, 1243–1249.

Shintani Y., Tanaka T., and Nozaki Y. (1997) GS-164, a small synthetic compound, stimulates tubulin polymerization by a similar mechanism to that of Taxol. *Cancer Chemother. Pharmacol.* **40**, 513–20.

Sigurdsson E. M., Lorens S. A., Hejna M. J., Dong X.-W., and Lee J. M. (1996) Local and distant histopathological effects of unilateral amyloid-$\beta_{15\text{-}35}$ injections into the amygdala of young F344 rats. *Neurobiol. Aging* **17**, 893–901.

Spillantini M. G., Murrell J. R., Goedert M., Farlow M. R., Klug A., and Ghetti B. (1998) Mutation in the tau gene in familial multiple system tauopathy with presenile dementia. *Proc. Natl. Acad. Sci. USA* **95**, 7737–7741.

Yankner B. A. (1996) Mechanisms of neuronal degeneration in Alzheimer's disease. *Neuron* **16**, 921–932.